

# An End-to-End BLE Indoor Location Estimation Method Using LSTM

Kenta Urano  
Graduate School of Engineering  
Nagoya University  
Aichi, Japan  
vrano@ucl.nuee.nagoya-u.ac.jp

Kei Hiroi  
Graduate School of Engineering  
Nagoya University  
Aichi, Japan

Takuro Yonezawa  
Graduate School of Engineering  
Nagoya University  
Aichi, Japan

Nobuo Kawaguchi  
Institutes of Innovation for Future Society  
Nagoya University  
Aichi, Japan

**Abstract**—Indoor location estimation has long been researched to realize location-based services. In this paper, we propose an indoor location estimation method for Bluetooth Low Energy (BLE) devices using end-to-end LSTM neural network. We focus on large-scale exhibition where is a tough environment for wireless indoor location estimation due to signal strength instability. To achieve higher accuracy, deep learning based methods are proposed rather than trilateration or fingerprint. Existing deep learning based methods estimate the location from the probabilities using the difference of query signal strength and autoencoder-reconstruction of it. Proposed method adopts end-to-end location estimation, which means the neural network takes a time-series of signal strength and outputs the estimated location at the latest time in the input time-series. We also build a loss function which takes how a person walks into account. Considering the difficulty of data collection within a short preparation term of an exhibition, the data generated by a simple simulation is used in the training phase before training with a small amount of real data. As a result, the estimation accuracy is average of 1.92m, using the data collected in GEXPO exhibition in Miraikan, Tokyo. Proposed method outperforms our previous trilateration based method's 4.51m average.

**Index Terms**—location estimation, BLE, deep learning, LSTM, end-to-end location estimation

## I. INTRODUCTION

To realize location-based services such as navigation to one's destination, information suggestion at appropriate timing and collection of marketing information, people's location is essential information. There are increasing demands on activity analysis of visitors at an indoor exhibition event (for example, walking trajectory, crowded area, and popular booth). Booth placement optimization and precise audience targeting in next year's event or a similar event require such information.

However, GPS signal, which is generally used outdoors, gets weaker and leads to inaccurate location detection. To solve this problem, indoor location estimation has long been researched. Among a variety of methods proposed, we focus on Bluetooth Low Energy (BLE) based location estimation.

BLE is ready-to-use with many devices such as smartphones, smartwatches, and IoT devices. Because BLE is designed to keep power consumption low for better battery life, we can use BLE devices for a long time without being bothered by battery shortage. We have been working on BLE location estimation for large-scale exhibition with mobile tag and fixed scanner style. This style makes the location estimation system simple because giving a BLE tag to a visitor is the only thing needed to start estimation.

The location estimation method in our previous research [1] was based on trilateration and particle filter. Calculation of existing probability at a certain location was done by trilateration with signal strength and the probability was used to resample the particles which represent the candidates of the estimated location.

The common problems of signal strength based location estimation are the fluctuation of signal due to noise and packet loss. Our previous method dealt with these problems by improving both on hardware and algorithm. Using tandem scanner which has multiple Bluetooth adapters and the algorithm which behavior can be controlled with parameters, higher accuracy was achieved. On the other hand, recent deep learning based location estimation methods are robust to noise and packet loss and reported to improve accuracy. Existing deep learning based methods adopts denoising autoencoder and estimates location based on the similarity of an input signal and the reconstructed signal.

In this paper, deep learning based end-to-end location estimation using BLE is proposed. End-to-end is, in this context, defined as that the neural network outputs the estimated location from the input signal strength. Proposed neural network takes a time-series of signal strength captured by the scanners in the area as input and outputs the estimated location at the latest time in the input time-series. The concept image of proposed end-to-end location estimation is shown in Fig.1. Fully connected layers and LSTMs are used in proposed neural network. We also use custom designed loss function which

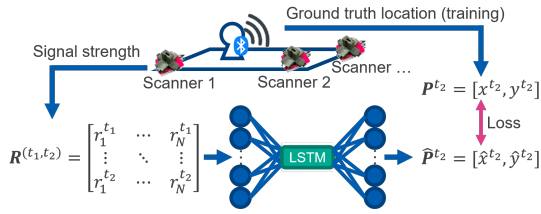


Fig. 1: Concept image of proposed end-to-end location estimation.

can evaluate several error components such as distance and direction to achieve higher accuracy. Because there are many possible network structure, to find the optimal structure, we evaluate estimation accuracy when changing the structure with the data collected in a real exhibition event.

Moreover, to decrease the amount of real data to train the neural network, a simple simulation of signal strength is adopted. This is because collecting a large amount of training data is difficult in the short preparation term of an event. As a result, training phase consist of two stages, the first stage with a vast amount of simulated data and the second stage with a small amount of real data.

In summary, this paper has the following contributions. (1) This paper presents an end-to-end location estimation method, from the time-series of BLE signal strength to the location with deep learning. Proposed method uses a custom design loss function to model the movement of a person for better accuracy. (2) Considering the difficulty of collecting the training data in a real environment, training of the neural network is done with simulated data and a small amount of real data. (3) Evaluation of the estimation accuracy when changing the layer configuration is performed to the data collected in a real exhibition event.

The remainder of this paper is organized as follows. In Section II, related location estimation methods are introduced. Proposed method is described in detail in Section III. The evaluation of estimation accuracy when changing the layer configuration of the neural network is performed in Section IV followed by the conclusions in Section V.

## II. RELATED WORK

There are many location estimation methods proposed with various approaches such as inertial sensor based [2], ultrasound based [3] and wireless communication based [4], [5]. Among many wireless communications (for example FM [6], RFID [7]) are used in location estimation, Wi-Fi [8] and BLE based methods are promising because of the rapid spread of smartphones and IoT devices. In this section, methods based on Wi-Fi and BLE are summarized by their estimation approach.

### A. Proximity

The proximity-based estimation uses the location of the device which recorded the strongest signal. This approach is straightforward and useful for area-level estimation. Komai et

al. [9] used this approach aiming to monitor what the residents do in the rooms of a nursing home.

### B. Distance or Angle Calculation

These methods estimate the location based on signal strength, Time of Flight (ToF), or Angle of Arrival (AoA). Signal strength is often used in the trilateration method which estimation is based on the distances from at least three devices. INTRI [10] employed the idea of forming contours surrounding the estimation target using the query signal strength and the signal strength collected in advance (like a fingerprint approach) for Wi-Fi location estimation rather than performing pure trilateration. Wang et al. [11] proposed trilateration based location estimation with Bluetooth devices. ToF needs accurate time sync among all devices. AoA needs antenna array or directional antenna. Wi-Fi Channel State Information (CSI) [12] is used in SpotFi [13] to estimate ToF and AoA. BLoC [14] defined Bluetooth CSI for location estimation while signal strength is the only information which we can get from Bluetooth signal in general.

### C. Fingerprint

To consider the environmental characteristics of signal strength (e.g. reflection, fading) fingerprint approach is widely used. This approach has two phases. In the training phase, reference fingerprint of signal strength is built through the measurement throughout the target environment. In the testing phase, pattern matching to the fingerprint is used to estimate the location from the query signal strength. For better accuracy or estimation speed, various fingerprint format and matching method are proposed [15]. RADAR [16] adopted Wi-Fi signal strength based fingerprint and matching based on neighborhoods in signal strength space. Wu et al. [17] focused on the similarity of Wi-Fi signal strength among adjacent locations and dealt with the instability of the signal. Faragher et al. [18] adopted fingerprint with fixed BLE tag and mobile scanner style location estimation.

### D. Deep learning based method

Recent success of deep learning enables higher accuracy location estimation. Current deep learning based methods adopt autoencoder as a neural network structure. Estimated location is basically calculated as a weighted average of fingerprint locations. The weight for each fingerprint location is calculated based on the similarity of the input and the output of autoencoder. Xiao et al. proposed DABIL [19] which estimates 3D location from BLE signal strength with denoising autoencoder. Denoising autoencoder is trained to restore missing values in the input and it is effective in the real environment with a lot of packet loss. In Wi-Fi location estimation, Wang et al. proposed DeepFi [20] which takes Wi-Fi CSI as the input for restricted Boltzmann machine. Another method WiDeep [21] proposed by Abbas et al. trained multiple autoencoders for robust estimation. Hoang et al. [22] focused on the relationship of the trajectory and the signal strength and proposed Recurrent neural network based Wi-Fi

location estimation. They compared multiple neural network configurations for better result.

### E. Limits of Existing Methods

Existing methods shown above have advantages and disadvantages. Proximity methods are simple but need dense installation of devices into the target environment for accurate estimation. Distance or angle calculation methods can keep the number of devices low, whereas signal noise affects estimated distance and angle. Fingerprint methods can realize accurate estimation, however, collecting a large amount of data throughout the target environment for training the model is tough labor.

When using deep learning, although we can expect robust and accurate estimation with a smaller number of devices, the same problem as fingerprint – collection of a large amount of training data – occurs. Moreover, existing deep learning based location estimation do not estimate location directly with a neural network. In this paper, we propose end-to-end location estimation with LSTM using time-series input. To mitigate the negative impact on estimation accuracy by the shortage of training data, simple simulation is used to generate the training data before training with a small amount of real data.

## III. PROPOSED END-TO-END LOCATION ESTIMATION

### A. Input and Output Data

To realize end-to-end location estimation, input data is signal strength captured by the scanners in the target environment. Using the signal strength  $r_i^t$  captured by the scanner  $i$  at time  $t$ , the set of signal strength  $\mathbf{R}^t$  can be described as (1). The total number of the scanners is referred to as  $N$ .

$$\mathbf{R}^t = (r_1^t, r_2^t, \dots, r_N^t) \quad (1)$$

However, in general,  $r_i^t$  is affected by noise or is unavailable due to packet loss. Because of that, only using  $\mathbf{R}^t$  as input makes the estimation difficult. Considering that the transition of signal strength has a relation with the movement of the person, time-series feature extraction can be used. Inputting time-series also helps the neural network to restore the missing value or remove the noise of signal strength. Therefore, proposed neural network takes the input with the shape shown in (2), which is a matrix of signal strength from time  $t_1$  to  $t_2$ .

$$\mathbf{R}^{(t_1, t_2)} = \begin{pmatrix} r_1^{t_1} & r_2^{t_1} & \dots & r_N^{t_1} \\ r_1^{(t_1+1)} & r_2^{(t_1+1)} & \dots & r_N^{(t_1+1)} \\ \vdots & \vdots & \ddots & \vdots \\ r_1^{t_2} & r_2^{t_2} & \dots & r_N^{t_2} \end{pmatrix} \quad (2)$$

The output is the estimated location at the time  $t_2$  which is the latest time in the input time-series. This estimated location  $\hat{\mathbf{P}}^{t_2}$  is 2D location as described in (3).

$$\hat{\mathbf{P}}^{t_2} = (\hat{x}^{t_2}, \hat{y}^{t_2}) \quad (3)$$

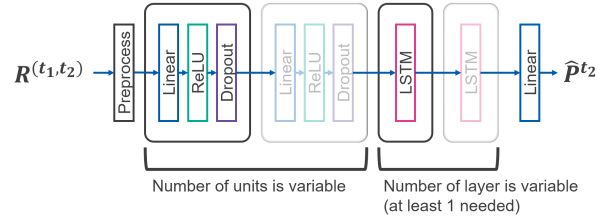


Fig. 2: Basic structure of proposed neural network.

### B. Neural Network Structure

The basic neural network structure is shown in Fig.2. Before inputting the data  $\mathbf{R}^{(t_1, t_2)}$  into the neural network, pre-processing is performed. In the preprocess all missing values are replaced with  $-100$  and then all values are shifted by  $+90$ . These values are empirically determined, through monitoring the change of training loss in several small experiments.

The preprocessed data is altered by fully connected (FC) units which consist of a linear layer, ReLU activation, and dropout. These FC units are expected to restore missing values and remove the noise. After the FC units, LSTMs are placed to extract the features in the time-series. The output of the last LSTM is processed by a linear layer to get the output  $\hat{\mathbf{P}}^{t_2}$ .

FC units and LSTMs can be repeated for changing the complexity of the neural network. The number of FC units can be zero, which means there is no correction on input data before LSTMs. The number of LSTMs is at least one because we need at least one LSTM to extract the features in the input. To find the optimal layer configuration, estimation accuracy when changing the numbers of FC units and LSTMs is evaluated in the next section.

### C. Loss Function

To get a better result in a noisy environment, the loss function is defined as (4) using the estimated location  $\hat{\mathbf{P}}^t$  and the ground truth locations  $\mathbf{P}^{t-1}$  and  $\mathbf{P}^t$ . In the equation,  $w_m$ ,  $w_c$  and  $w_r$  are the weights of the terms.  $\text{Cos}()$  returns cosine similarity of input vectors.  $D$  and  $\hat{D}$  are described as (5) and (6) respectively. They correspond to the distance from  $\mathbf{P}^{t-1}$ .

$$L(\hat{\mathbf{P}}^t, \mathbf{P}^{t-1}, \mathbf{P}^t) = w_m \text{MSE}(\hat{\mathbf{P}}^t, \mathbf{P}^t) + w_c D(1 - \text{Cos}(\mathbf{P}^t - \mathbf{P}^{t-1}, \hat{\mathbf{P}}^t - \mathbf{P}^{t-1})) + w_r \text{ReLU}(\hat{D} - D) \quad (4)$$

$$D = \text{Distance}(\mathbf{P}^t, \mathbf{P}^{t-1}) \quad (5)$$

$$\hat{D} = \text{Distance}(\hat{\mathbf{P}}^t, \mathbf{P}^{t-1}) \quad (6)$$

This loss function consists of three terms. The first MSE term corresponds to the distance between the estimated location and the ground truth location. This term just means that the distance error should be small.

The second term corresponds to the direction difference of the estimated location  $\hat{\mathbf{P}}^t$  and the ground truth location  $\mathbf{P}^t$ , based on the ground truth location  $\mathbf{P}^{t-1}$ . The latter part produces 0 when  $\mathbf{P}^t$  and  $\hat{\mathbf{P}}^t$  head for the same direction. The

value of this term also changes depending on the distance of ground truth locations,  $D$ . The intuitions behind this term are as follows. (1) This term should react sharply to the direction error when  $D$  is large. This is because even if the direction error is small, a large error occurs with long distance. (2) When  $D$  is small, a large direction error does not lead to large location error. Therefore, this term does not charge a large penalty.

The third term is for avoiding the leap of the estimated location. When the estimated location goes farther than the ground truth location, ReLU is activated to place the additional penalty.

#### D. Training with Simulated and Real Data

Collecting the training data is an inevitable problem with deep learning based method. The difficulty of data collection at an exhibition event is greater than that at a permanent installation case due to the following reasons.

- Short preparation time – Booth construction time, which we can use for data collection is very limited. Moreover, signal propagation changes during the construction of booths.
- Gap of signal strength – Signal strength is different between preparation time and exhibition time due to visitors. There is greater noise when many visitors are wandering.

To train the neural network with a small amount of real data, we use the signal strength data generated by a simple simulation. This idea is related to data augmentation, although we generate the data instead of modifying real data. The procedure of the data generation is as follows.

- 1) Randomly choose a location  $P_1$  in the target area.
- 2) Within a certain distance from  $P_1$ , randomly choose another location  $P_2$ .
- 3) Calculate how distances from the scanners change when the person moves from  $P_1$  to  $P_2$ .
- 4) Calculate ideal signal strength which should be recorded by each scanner in the area based on the distances calculated in the previous step.
- 5) Add random value sampled from a normal distribution as the signal noise to the signal strength.
- 6) Replace some values with  $-100$  based on predefined probability. This operation corresponds to packet loss.

In step 4, the set of ideal signal strength  $R_{ideal}^t$  is described as (7) using the set of distances  $d^t = (d_1^t, d_2^t, \dots, d_N^t)$  to the person from the scanners. In (7),  $tx$  corresponds to the transmission power which should be recorded when the distance of a BLE tag and a scanner is 1m and  $n$  corresponds to the attenuation constant which models how lossy the signal is in the target environment.

$$R_{ideal}^t = tx - 10n \log_{10} d^t \quad (7)$$

In step 5, a set of random variables  $n_N$  is added to  $R_{ideal}^t$  as described in (8).  $n_N$  is sampled from a normal distribution with predefined mean and standard deviation. This step models

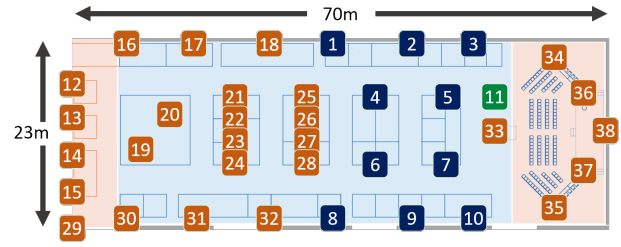


Fig. 3: Locations of the installed scanners.

TABLE I: Common neural network parameters of all configurations.

Parameter	Value
Length of input time-series	10s
Number of scanners $N$	38
Dropout probability	0.3
Number of LSTM hidden state	64
Weights of loss function $w_m, w_c, w_r$	1, 10, 5
Optimization	Adagrad

the noise which occurs due to the presence of visitors and booths.

$$R_{noise}^t = R_{ideal}^t + n_N \quad (8)$$

After that, in step 6, some values of  $R_{noise}^t$  are replaced to  $-100$  (which means missing value) based on the probability  $p_{drop}$  as shown in (9). This operation models packet loss.

$$R_{drop}^t = f_{drop}(R_{noise}^t; p_{drop}) = (-100, r_2^t, r_3^t, -100, -100, \dots, r_N^t) \quad (9)$$

## IV. EVALUATION OF ESTIMATION ACCURACY

As stated in the previous section, estimation accuracy when changing the number of layers is evaluated in this section. 10 patterns of configurations are tested – FC: 0, 1, 2, 3, 4 and LSTM: 1, 2. Larger number of FC means the neural network will correct signal strength more strongly before LSTM. Single LSTM extracts the features of time-series and double LSTMs extract the features of the change of time-series.

### A. Target environment

*Data Collection:* The data used in the evaluation is from the experiment at GEXPO2016 exhibition held in Miraikan museum, Tokyo, Japan. The exhibition was a 3-day exhibition aiming to promote the active use of geospatial technology. The number of total visitors was 19,138. In the experiment, 38 scanners were installed in the exhibition area (70m  $\times$  23m) as shown in Fig.3.

Experiment subject wore a BLE tag and a UWB (Ultra Wide-Band) tag (for recording the ground truth) at the entrance and moved freely. We collected the data from a total of 260 subjects in the exhibition.

TABLE II: Parameters of simulated data generation.

Parameter	Value
Number of scanners	38
Area size	70m × 23m
Length of time-series	10s
Distance of $P_1$ and $P_2$	10m <sup>1</sup>
Transmission power $tx$	-59 <sup>2</sup>
Attenuation constant $n$	2.0
Noise mean	-5
Noise standard deviation	4
Packet loss prob. $p_{drop}$	0.85 <sup>3</sup>

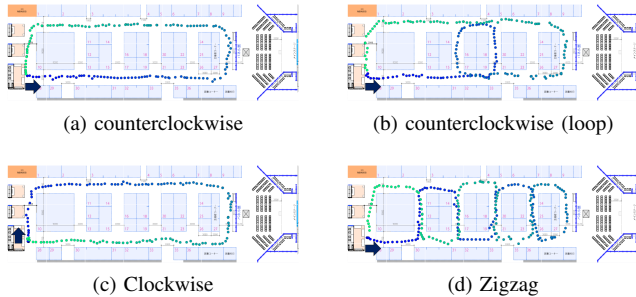


Fig. 4: Paths for testing.

*Training and Testing:* As stated in the previous section, simulated data is used as well as real experiment data to train the neural network. The common neural network parameters of all configurations are shown in Table I.

The simulated data with the amount of 160,000 is generated for training with the parameters shown in Table II. Training with this simulated data is done for 200 epochs with a batch size of 100.

Additional training with the real data follows the training with the simulated data. From GEXPO2016 experiment data, the records of 20 subjects are used. Each record is converted into 10-second slices using the sliding window with 1-second slide width. Because the beaconing frequency of the BLE tags used in the experiment was 10Hz, maximum signal strength is extracted when multiple signal readings are available in one second for a scanner. The total amount of the data for the additional training is 78,000. Additional training is done for 100 epochs with a batch size of 100.

The data for testing is from the records of 3 subjects which are not included in the data for the additional training. These subjects walked four paths which are shown in Fig.4. For all paths, the subjects walked from the experiment desk to the direction shown by the arrow marks and returned to the desk. The same conversion with the additional training data is performed to feed the data to the neural network.

<sup>1</sup>The subject is assumed to walk at 1m/s.

<sup>2</sup>This value was set to the BLE tags used in the experiment.

<sup>3</sup>Empirically determined, assuming that the scanners about 10m away from the subject can receive packets, through monitoring the change of training loss in several small experiments.

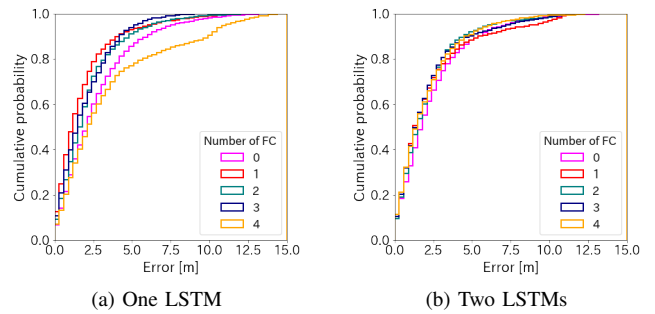


Fig. 5: Cumulative probability and error.

TABLE III: Error at cumulative probability of 0.5, 0.75, 0.9

FC units	LSTM	Error at cum. prob.[m]		
		p=0.5	p=0.75	p=0.9
0	1	2.19	3.83	6.15
1		<b>1.30</b>	<b>2.44</b>	<b>4.26</b>
2		1.80	2.88	4.94
3		1.60	3.07	4.39
4		2.36	4.59	10.1
0	2	1.87	3.37	5.70
1		1.48	2.97	5.70
2		1.66	2.93	4.62
3		1.51	2.85	4.95
4		1.56	3.02	4.83

### B. Quantative Result

For all configurations, training and testing are performed. Fig.5 shows the cumulative probabilities and estimation errors of all configurations. Fig.5a and Fig.5b illustrates the results of the configurations with one LSTM and the results of the configurations with two LSTMs, respectively. Table III shows the error when cumulative probabilities are 0.5, 0.75, 0.9. Table IV shows the error average and standard deviation (SD) of each configuration.

From Fig.5a and Table III, when using one LSTM, the results clearly degrade when using 0 FC and 4 FCs. When using two LSTMs, as shown in Fig.5b, there is little difference among the configurations. From Table III, the configuration of one FC and one LSTM achieved the lowest error at the all cumulative probabilities of 0.5, 0.75, 0.9. Table IV shows that there is little difference both in error average and error SD among almost all configurations. Considering these results and the idea that a simpler model is better when several models report the same result, the configuration with one FC and one LSTM is the best with average error of 1.92m in this experiment. This result outperforms the average of 4.51m which is the best result of our previous trilateration based location estimation.

### C. Qualitative Result

From the quantitative result, estimation accuracy is not much different regardless of layer configuration. Therefore the examples of the qualitative result are shown here. Fig.6 shows the examples of ground truth locations and the estimated locations plotted on the map of the target environment.

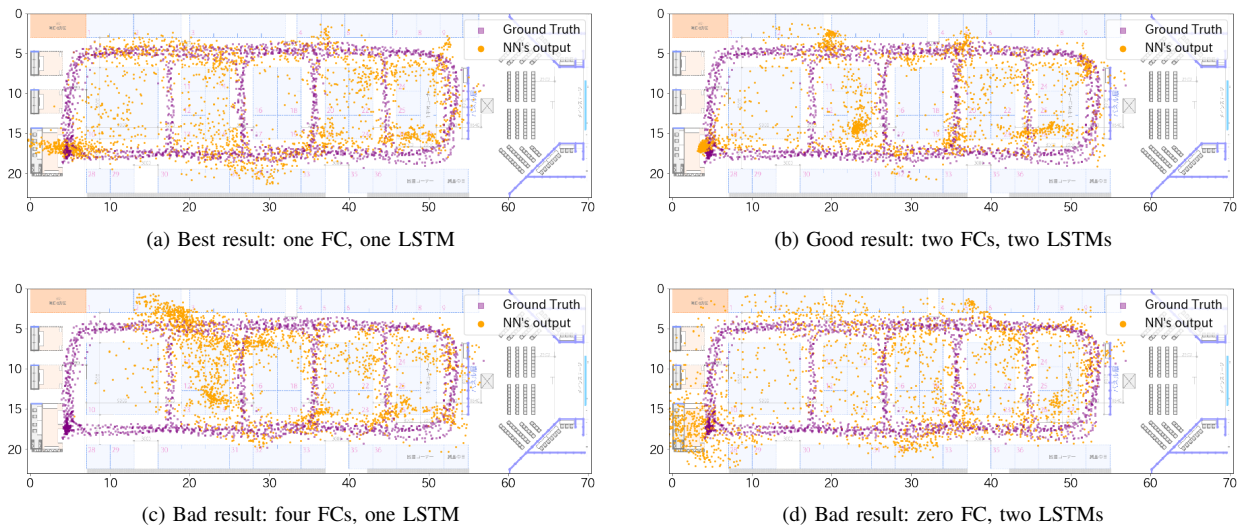


Fig. 6: Distributions of estimated locations by different configurations.

TABLE IV: Error average and standard deviation (SD)

FC units	LSTM	Error average [m]	Error SD [m]
0	1	2.83	3.47
1		<b>1.92</b>	2.05
2		2.27	2.05
3		2.07	<b>1.74</b>
4		3.62	3.52
0	2	2.53	2.38
1		2.39	2.56
2		2.20	2.11
3		2.22	2.27
4		2.20	2.19

According to Table III, Fig.6a illustrates the best result and Fig.6b illustrates a good result. Fig.6c and 6d illustrate bad results.

In Fig.6c, estimation on the most left part of the area is not successful. All configurations with two LSTMs produced the estimated locations gathering to some locations like shown in Fig.6b, except zero FC configuration (Fig.6d). From Fig.6a, the estimated locations fluctuate rather than align to the ground truth even in the best result. This tendency can be seen in the standard deviation shown in Table IV. Therefore additional consideration is needed to the neural network structure or the loss function, for example, loss based on the quality of corrected signal strength.

## V. CONCLUSIONS

In this paper, we proposed an end-to-end BLE indoor location estimation method which adopts LSTM neural network. The neural network of proposed method takes the time-series of signal strength captured by the scanners in the target environment as input and outputs the estimated location at the latest time in the input. For higher estimation accuracy, loss function is designed to model the movement of a person. Aiming to use at a large-scale exhibition where exhaustive

data collection is difficult, simulation data is used to train the neural network as well as a small amount of real data.

Evaluation of estimation accuracy by changing the number of layers is performed to find the optimal neural network structure. As a result, one FC and one LSTM is found to be the best configuration with an average error of 1.92m. However, from the qualitative result, estimated locations do not align well to the ground truth.

In conclusion, proposed neural network can estimate the location of the person in the exhibition. However, the following three things need to be investigated and improved to achieve an accurate and robust result. Firstly, simulated data for training should be more realistic. Simple signal strength calculation and noise from a normal distribution are used to generate the simulated data in this paper, however, an analysis of the distribution of signal strength and noise will lead to better simulation. Secondly, estimation accuracy when changing the amount of simulated and real training data should be investigated to reveal the effect of the presence of the simulated data. The extreme case will be no simulated data or no real data for training. Thirdly, this system should be tested in various environments (for example, museum and office building). Another environment has different signal propagation characteristics and estimation accuracy will change.

## REFERENCES

- [1] Kenta Urano, Katsuhiko Kaji, Kei Hiroi, and Nobuo Kawaguchi. A Location Estimation Method Using Mobile BLE Tags with Tandem Scanners. In *5th International Workshop on Human Activity Sensing Corpus and Application (HASCA2017)*, pages 577–586, 2017.
- [2] Stéphane Beauregard and Harald Haas. Pedestrian Dead Reckoning: A Basis for Personal Positioning. In *3rd Workshop on Positioning, Navigation and Communication*, pages 27–35, 2006.
- [3] Mike Hazas and Andy Hopper. Broadband Ultrasonic Location Systems for Improved Indoor Positioning. *IEEE Transactions on Mobile Computing*, 5(5):536–547, 2006.
- [4] Hui Liu, Houshang Darabi, Pat Banerjee, and Jing Liu. Survey of Wireless Indoor Positioning Techniques and Systems. *IEEE Transactions on Systems, Man, and Cybernetics, Part C (Applications and Reviews)*, 37(6):1067–1080, 2007.

- [5] Yanying Gu, Anthony Lo, and Ignas Niemegeers. A Survey of Indoor Positioning Systems for Wireless Personal Networks. *IEEE Communications Surveys & Tutorials*, 11(1):13–32, 2009.
- [6] Yin Chen, Dimitrios Lymberopoulos, Jie Liu, and Bodhi Priyantha. Fm-based indoor localization. In *10th International Conference on Mobile Systems, Applications, and Services (MobiSys '12)*, pages 169–182, 2012.
- [7] Lionel M. Ni, Yunhao Liu, Yiu Cho Lau, and Abhishek P. Patil. LANDMARC: Indoor Location Sensing using Active RFID. In *1st IEEE International Conference on Pervasive Computing and Communications (PerCom 2003)*, pages 407–415, 2003.
- [8] A. Khalajmehrabadi, N. Gatsis, and D. Akopian. Modern WLAN Fingerprinting Indoor Positioning Methods and Deployment Challenges. *IEEE Communications Surveys & Tutorials*, 19(3):1974–2002, thirdquarter 2017.
- [9] Kiyooki Komai, Manato Fujimoto, Yutaka Arakawa, Hirohiko Suwa, Yukitoshi Kashimoto, and Keiichi Yasumoto. Beacon-Based Multi-Person Activity Monitoring System for Day Care Center. In *IEEE International Conference on Pervasive Computing and Communication Workshops (PerCom Workshops)*, pages 1–6, 2016.
- [10] Suining He, Tianyang Hu, and Shueng-Han Gary Chan. Contour-based Trilateration for Indoor Fingerprinting Localization. In *13th ACM Conference on Embedded Networked Sensor Systems (SenSys '15)*, pages 225–238, 2015.
- [11] Yapeng Wang, Xu Yang, Yutian Zhao, Yue Liu, and Laurie Cuthbert. Bluetooth Positioning Using RSSI and Triangulation Methods. In *IEEE 10th Consumer Communications and Networking Conference (CCNC)*, pages 837–842, 2013.
- [12] Daniel Halperin, Wenjun Hu, Anmol Sheth, and David Wetherall. Tool Release: Gathering 802.11n Traces with Channel State Information. *SIGCOMM Computer Communication Review*, 41(1):53–53, 2011.
- [13] Manikanta Kotaru, Kiran Joshi, Dinesh Bharadia, and Sachin Katti. SpotFi: Decimeter Level Localization using WiFi. In *ACM Conference on Special Interest Group on Data Communication (SIGCOMM '15)*, pages 269–282, 2015.
- [14] Roshan Ayyalasomayajula, Deepak Vasisht, and Dinesh Bharadia. BLoc: CSI-based Accurate Localization for BLE Tags. In *14th International Conference on Emerging Networking EXperiments and Technologies (CoNEXT '18)*, pages 126–138, 2018.
- [15] Suining He and Shueng-Han Gary Chan. Wi-Fi Fingerprint-Based Indoor Positioning: Recent Advances and Comparisons. *IEEE Communications Surveys & Tutorials*, 18(1):466–490, 2016.
- [16] Paramvir Bahl and Venkata N Padmanabhan. RADAR: An In-building RF-based User Location and Tracking System. In *19th Annual Joint Conference of the IEEE Computer and Communications Societies (INFOCOM 2000)*, pages 775–784, 2000.
- [17] Chenshu Wu, Jingao Xu, Zheng Yang, Nicholas D. Lane, and Zuwei Yin. Gain Without Pain: Accurate WiFi-based Localization Using Fingerprint Spatial Gradient. *Proceedings of the ACM on Interactive, Mobile, Wearable Ubiquitous Technologies*, 1(2):29:1–29:19, June 2017.
- [18] Ramsey Faragher and Robert Harle. Location Fingerprinting With Bluetooth Low Energy Beacons. *IEEE journal on Selected Areas in Communications*, 33(11):2418–2428, 2015.
- [19] Chao Xiao, Daiqin Yang, Zhenhong Chen, and Guang Tan. 3-D BLE Indoor Localization Based on Denoising Autoencoder. *IEEE Access*, 5:12751–12760, 2017.
- [20] Xuyu Wang, Lingjun Gao, Shiwen Mao, and Santosh Pandey. DeepFi: Deep Learning for Indoor Fingerprinting using Channel State Information. In *IEEE Wireless Communications and Networking Conference (WCNC)*, pages 1666–1671, 2015.
- [21] Moustafa Abbas, Moustafa Elhamshary, Hamada Rizk, Marwan Torki, and Moustafa Youssef. WiDeep: WiFi-based Accurate and Robust Indoor Localization System using Deep Learning. In *17th IEEE International Conference on Pervasive Computing and Communications (PerCom 2019)*, pages 232–241, 2019.
- [22] Minh Tu Hoang, Brosnan Yuen, Xiaodai Dong, Tao Lu, Robert Westendorp, and Kishore Reddy. Recurrent Neural Networks For Accurate RSSI Indoor Localization. In *arXiv:1903.11703*, pages 1–10, 2019.